IEEE Access
Multidisciplinary | Rapid Review | Open Access Journal

Received July 18, 2019, accepted July 25, 2019, date of publication August 1, 2019, date of current version August 16, 2019.

Digital Object Identifier 10.1109/ACCESS.2019.2932383

Design and Test of 4.6 GHz 500 kW Continuous Wave 3 dB High Power Divider

DINGZHEN LI[1,2], (Member, IEEE), LIANMIN ZHAO[1], FUKUN LIU[1], HUA JIA[1], MIN CHENG[1], XINSHENG YAN[1,2], AND TAIAN ZHOU[1]

[1]Institute of Plasma Physics, Chinese Academy of Sciences, Hefei 230031, China
[2]University of Science and Technology of China, Hefei 230026, China

Corresponding author: Lianmin Zhao (lmzh@ipp.ac.cn)

This work was supported in part by the National MCF Energy Research and Development Program of China under Grant 2018YFE0305100, and in part by the National Natural Science Foundation of China under Grant 11675212.

ABSTRACT A 500-kW continuous-wave (CW) high-power 3-dB divider is designed for the 4.6-GHz lower hybrid current drive system in the Experimental and Advanced Superconducting Tokamak (EAST). A multi-stepped structure is used to increase the power capacity, and a water cooling structure is introduced to reduce the thermal deformation and gas breakdown, which keeps the maximum steady-state temperature of the divider below 60 °C under full-power (500 kW) operation. The result of the simulations of the electric field shows that the power capacity of the multi-stepped structure is more than twice compared with the traditional design. Moreover, the divider shows excellent performance in the low-power test, with low return loss (−35 dB) and similar division ratio ($S_{21} = -3.004$ dB and $S_{31} = -3.035$ dB) at 4.6 GHz. Both the division ratio test and the full reflection test were carried out successfully under 250-kW CW, which suggests that the development of the 3-dB divider satisfies the design requirements.

INDEX TERMS High power, multi-stepped, power capacity, steady-state thermal analysis.

I. INTRODUCTION

Power dividers are key components of lower hybrid current drive (LHCD) systems on Tokamaks, such as the 2.45 GHz LHCD system in EAST [1], 3.7 GHz LHCD systems in HL-2A [2], [3], ADITYA-Upgrade tokamak [4] and SST1 [5], 5 GHz LHCD systems in K-STAR [6] and ITER [7]. Some dividers are operating under high power short pulses (500 kW 2s [2], [3]), others are operating under lower power CW (250kW [4] or 300kW [6]). However, for futural 4.6 GHz 500 kW LHCD system, an integrated design of the power divider with both high power and CW must be developed.

In the present 4.6 GHz LHCD system in the Experimental and Advanced Superconducting Tokamak (EAST), the maximum power capacity of the 3 dB divider is 250 kW, since a tuning pin is used in the coupling area to adjust the input port matching and the power division ratio. However, the pin would cause the electric field increased around itself. For high power CW, the presence of the pin would limit the power capacity, which depends on the amplitude of the electrical field. Therefore, one of the design challenges is how to remove the pin while keeping the transmission and division performance of the device. Besides, the thermal effects of high-power microwave device under steady-state operation cannot be ignored. On the one hand, a rise in the temperature of the power divider would cause arcing inside it as it lowers the electrical field threshold breakdown, on the other hand, the thermal deformation of the divider would increase the voltage standing wave ratio (VSWR) and reduce the power capacity.

In section II, this work aim to calculate the physical size and transmission loss of the divider, analyze the thermal effect of the components and build a water cooling structure to maintain the steady state operation. And the power capacity is calculated based on the temperature distribution of the device. Section III introduces the experiment and the high power test of the 3 dB divider. Finally, a brief conclusion is given.

The associate editor coordinating the review of this manuscript and approving it for publication was Andrei Muller.

II. DESIGN OF THE 3 dB DIVIDER

A. RF TRANSMISSION ANALYSIS

As shown in Fig 1, The power divider consists of four WR229 rectangular waveguides (58.2 mm × 29.1 mm) and one coupling area. In this device the microwave input from

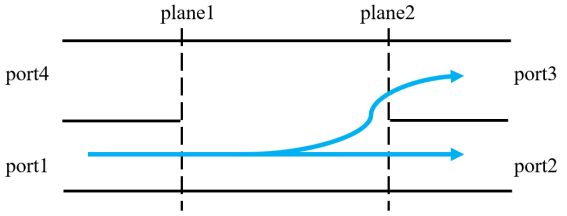

FIGURE 1. Simplified structure of the 3 dB power divider [3].

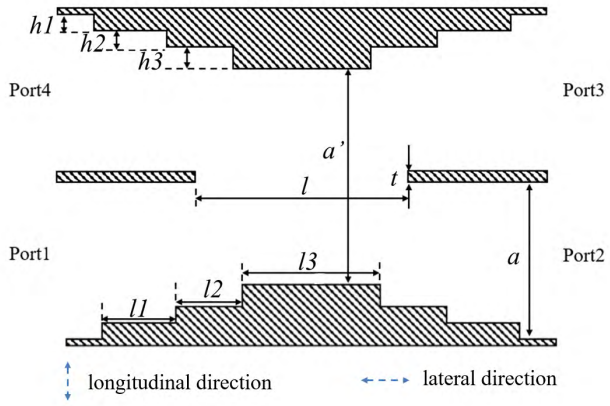

FIGURE 2. Actual power divider structure.

port 1 is equally divided into output port 2 and port 3, yet the phase difference between these two ports is 90°, while port 4 is used as the isolated port. According to the symmetry and the reciprocity, the scattering matrix of the power divider can be written as

$$[S] = \frac{1}{\sqrt{2}} \begin{bmatrix} 0 & 1 & \mathrm{j} & 0 \\ 1 & 0 & 0 & \mathrm{j} \\ \mathrm{j} & 0 & 0 & 1 \\ 0 & \mathrm{j} & 1 & 0 \end{bmatrix}$$

The propagation modes of the divider are the TE_{10} mode and the TE_{20} mode. The TE_{30} mode and higher order modes should be cut off. The TE_{10} and the TE_{20} modes are generated by odd and even modes excitation, respectively. The cutoff wavelength [8] of the TE_{30} mode in the coupling cavity portion can be calculated as

$$\lambda_{cTE_{30}} = \frac{2}{\sqrt{\left(\frac{3}{2a}\right)^2 + \left(\frac{0}{b}\right)^2}} = \frac{4}{3}a = 77.56\text{mm} \quad (1)$$

where a and b are the length and width of the waveguide cutting plane, respectively. The operating wavelength of the 4.6 GHz electromagnetic wave is 65.2 mm, indicating that the TE_{30} mode could be transmitted in the coupling area. Thus, the sizes of the coupling area especially the height a' must be reduced to suppress the TE_{30} mode. For this, a multi-stepped structure is adopted by adding three steps in the coupling area to adjust the size of the waveguide. The actual divider structure is shown in Fig. 2:

To guarantee that the TE_{30} mode is cut off and the TE_{20} mode is transmitted, the λ should be satisfied

$$\begin{cases} \lambda'_{\mathrm{cTE}_{30}} = \dfrac{2}{\sqrt{\left(\frac{3}{a'}\right)^2 + \left(\frac{0}{b}\right)^2}} = \dfrac{2}{3}a' < \lambda \\ \lambda'_{\mathrm{cTE}_{20}} = \dfrac{2}{\sqrt{\left(\frac{2}{a'}\right)^2 + \left(\frac{0}{b}\right)^2}} = a' > \lambda \end{cases} \quad (2)$$

where a' is the height of the coupling area, and Eq. (2) is solved as 65.2 mm < a' < 97.8 mm, and the scattering parameters of the above network [9], [10] can be calculated by

$$\begin{cases} S_{21} = \cos[\dfrac{1}{2}(\beta_e - \beta_o)\, l]e^{-\mathrm{j}\frac{1}{2}(\beta_e+\beta_o)l} \\ S_{31} = \mathrm{j}\cos[\dfrac{1}{2}(\beta_e + \beta_o)\, l]e^{-\mathrm{j}\frac{1}{2}(\beta_e+\beta_o)l} \end{cases} \quad (3)$$

where β_e, β_o are the wave numbers of the even mode and the odd mode [8], respectively. In order to guarantee the same electric field amplitude in the two ports, the following expression should be satisfied.

$$\frac{1}{2}(\beta_e - \beta_o)\, l = \frac{\pi}{4}. \quad (4)$$

Setting a' as 80 mm, the solution of Eq. 4 led to dimension of l = 48.8 mm. The other structure parameters were optimized with CST Microwave Studio are displayed in Table 1.

TABLE 1. Dimensions of the 4.6 GHz 500 kW power divider.

h_1 [mm]	6.8
h_2 [mm]	7.1
h_3 [mm]	6.8
l_1 [mm]	12.9
l_2 [mm]	13.2
l_3 [mm]	30.6
t [mm]	6

Since the two parallel ports of the divider need to be separated for actual facilitate installation, in the CST Microwave Studio model, each port was stretched for 100 mm in the lateral direction (the propagating direction of the wave, see Fig. 2) and 30 mm in the longitudinal direction (the wide side of the waveguide, see Fig. 2). The amplitude and phase of electric field in the resulting divider with the input power of 500 kW is shown in Fig. 3. It is seen that the power input from port 1 is evenly distributed to port 2 and port 3. Moreover, as shown in Fig. 4, the phase difference between port 2 and port 3 is precisely 90° at 4.6 GHz.

The transmission loss of rectangular waveguide is mainly resulted from the conductor loss, and for TE_{10} mode, it can be found by using formula [8]

$$\alpha_c = \frac{R_s}{a^3 b\beta k\eta}(2b\pi^2 + a^3k^2)\text{Np/m} \quad (5)$$

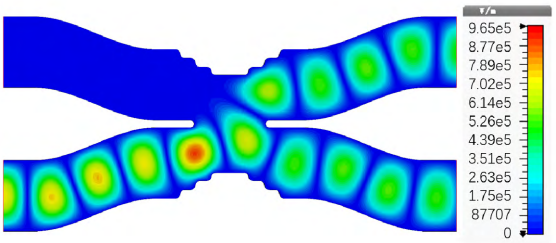

FIGURE 3. Electric field in the divider considering a 500 kW excitation in CST.

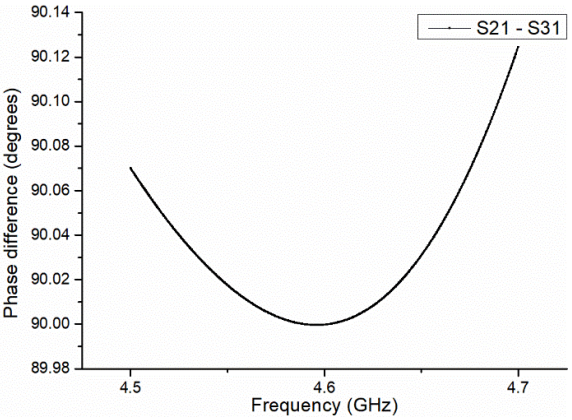

FIGURE 4. Phase difference between port 2 and port 3.

where k is the wavenumber, $R_s = \sqrt{\omega\mu_0}/(2\sigma)$ is the surface resistivity of the waveguide and $\omega = 2\pi \times 4.6 \times 10^9 \mathrm{rad/s}$, $\mu_0 = 4\pi \times 10^{-7} \mathrm{N/A^2}$ and $\sigma = 5.8 \times 10^7 \mathrm{S/m}$ are the operating frequency, permeability of vacuum and conductivity of copper [11], respectively. And copper is the material of the divider. The transmission loss of the TE_{20} mode is substituted with the transmission loss of the TE_{10} mode to simplify the calculation. The wave would propagate at most 0.39 m in the divider, so the loss could be calculated as 984.3 W nearly.

B. STEADY-STATE THERMAL ANALYSIS

The steady-state thermal analysis is performed with ANSYS workbench considering the air convection with the environmental temperature of 20 °C and the related results are shown in Fig. 5. It shows that when the surface temperature of the waveguide has stabilized, the maximum temperature is nearly 301 °C, and the lowest temperature is nearly 293 °C. Set the back surface of the divider as the fixed support, then the maximum deformation (681 um) of the divider would locate at the ports of the front wall. The waveguide may be thermally deformed because of the high temperature, which would decrease the power capacity of the divider. Additional cooling structures are indispensable.

The divider would be cooled by water flowing through a rectangular copper pipe with a section of 10 mm × 5 mm, is placed along the surface of the waveguide, the main properties of copper are reported in Table 2.

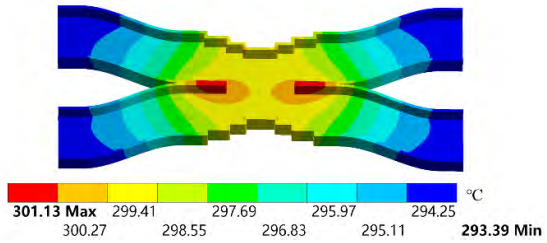

(a)

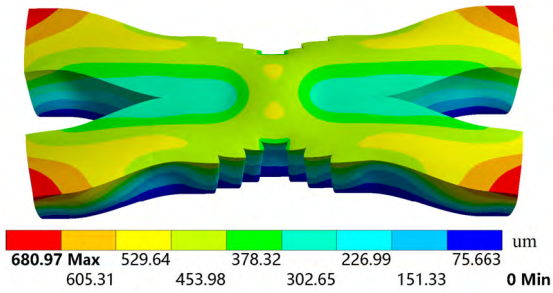

(b)

FIGURE 5. Steady-state thermal analysis: (a) temperature distribution; (b) total deformation.

TABLE 2. Main properties of copper.

Property	Value
Density (kg/m^3)	8850
Isotropic Thermal Conductivity (W/(m·K))	243
Specific Heat (J/(kg·K))	385

TABLE 3. Main thermal physical properties of water at 20 °C and 40 °C.

T(°C)	tc(W/(m·K))	η (kg/(m·s))	v (m^2/s)	Pr
20	59.9×10^{-2}	1004×10^{-6}	1.006×10^{-6}	7.02
40	63.5×10^{-2}	653.3×10^{-6}	0.659×10^{-6}	4.31

The equivalent diameter of the pipe d_e can be calculated as

$$d_e = \frac{4A_c}{p} = 6.7\mathrm{mm} \tag{6}$$

where A_c and p are the area and perimeter of the cross section.

According the requirements of the LHCD system in EAST, the temperature difference between the inlet water and the outlet water should be less than 20 °C. Since the initial water temperature is set as 20 °C, the temperature of the outlet water should be closed to 40 °C. In addition, the mass flow rate of the water system is set as 0.1 kg/s, which led the water velocity u to 2 m/s. The main thermal physical properties of water are reported in Table 3. Where tc, η, v, Pr are thermal conductivity, dynamic viscosity, thermal diffusivity and Prandtl Number.

The Reynolds number [12] can be calculated by

$$Re_f = \frac{u \cdot d_e}{\nu_f} = 1.332 \times 10^4 \tag{7}$$

According to Sieder-Tate formula, the Nusselt number [12] can be calculated by

$$Nu = 0.027 R_e^{0.8} Pr_f^{1/3} \left(\frac{\eta_f}{\eta_w}\right)^{0.14} \tag{8}$$

where the subscripts f and w respectively indicate that the water temperature is 20 °C and 40 °C, respectively. The convective heat transfer coefficient [12] of water is

$$h = \frac{tc_f}{d_e} Nu = 9509 \text{W/(m}^2 \cdot \text{K)} \tag{9}$$

Setting the heat transfer coefficient to 9509 W/(m2 · K) at the connection interface between the divider and pipe in ANSYS workbench, and the result of steady-state thermal analysis of the divider with water cooling structure is portrayed in Fig. 6. It shows that the maximum surface temperature of the waveguide (∼55 °C) is at the ports, and at the coupling area with water cooling, where the maximum electric field locates (see Fig. 3), the temperature of the divider is below 40 °C, satisfying the design requirements.

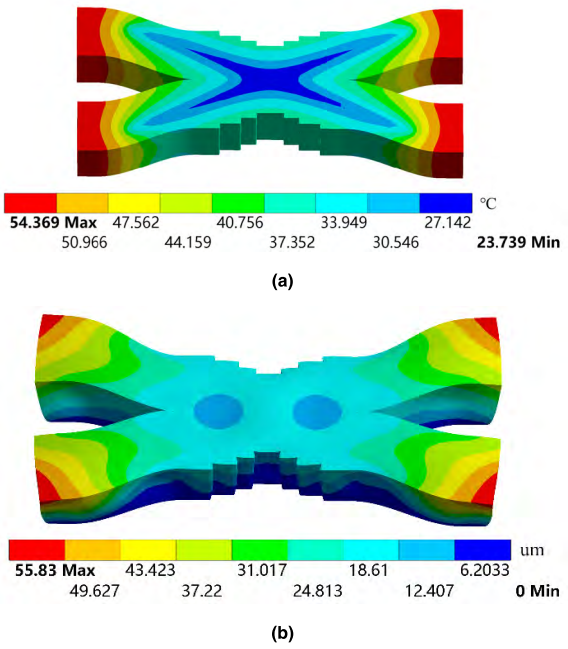

FIGURE 6. Steady-state thermal analysis with water cooling structure: (a) temperature distribution; (b) total deformation.

C. POWER CAPACITY CALCULATION

The prevention of microwave breakdown is a serious challenge in high power operations [13]–[17]. Microwave breakdown in undissociated air is caused by the ionization of neutral molecules by free electrons that have acquired sufficient energy from interactions with the electric field and the gas particles. As the waveguide temperature rises, decreasing of the critical electric field of the air breakdown inside the waveguide is the main factor limiting the power capacity of the waveguide.

An in-depth study [13] on microwave breakdown of air-filled waveguide shows that the critical breakdown field EB can be calculated by

$$\left(\frac{E_B}{p^*}\right)_{p^*\lambda \neq 0} = \left(\frac{E_B}{p^*}\right)_{p^*\lambda = 0} - \Delta\left(p^*\lambda\right) \tag{10}$$

where p^* and $\Delta(p^*\lambda)$ may be approximated by

$$p^* = \left(298/T_a\right)(760)\ \text{Torr} \tag{11}$$

$$\Delta(p^*\lambda) \approx 6[1 - \exp(-0.75 \times 10^{-3} p^*\lambda)] \tag{12}$$

where T_a is the air temperature and λ is the wavelength. So the critical electric field for breakdown would be 18.7 kV/cm at 4.6 GHz when the temperature is 40 °C and the atmospheric pressure is 760 Torr (1.01×10^5 Pa).

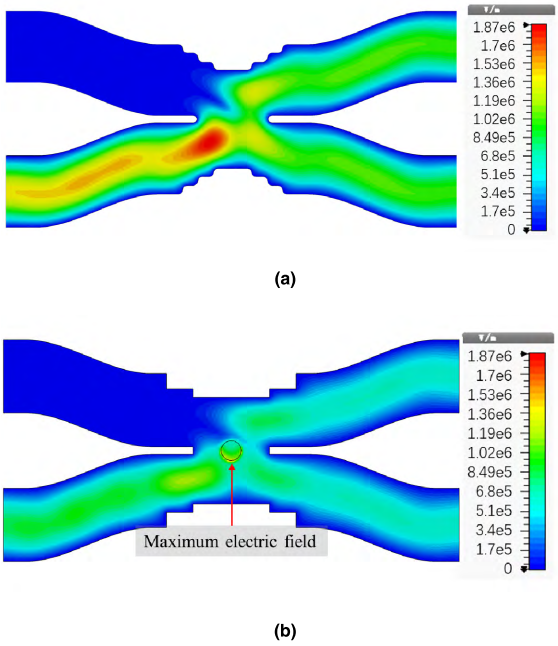

FIGURE 7. Amplitude of electric field on two 3 dB dividers: (a) multi-stepped divider with 1.876 MW input power; (b) traditional divider with 681.3 kW input power.

Fig. 7 shows the simulated amplitudes of the electric fields in the multi-stepped divider and the traditional divider with the maximum electric field of 18.7 kV/cm. Note that, in the simulation, the input power in the multi-stepped divider is 1.876 MW whereas the power in the traditional divider with pin is only 681.3 kW, implying that the power capacity is more than twice during matched condition after removing the pin. Since the transmission power must be less than one third of the power capacity [8], the traditional power divider does not satisfy the design requirements.

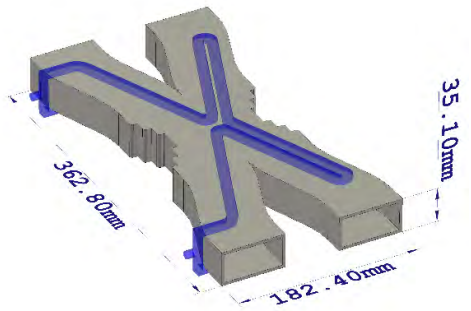

(a)

(b)

FIGURE 8. Model of the divider: (a) 3D model; (b) photograph.

III. TEST OF THE 3 dB DIVIDER

A. LOW-POWER TEST

Based on above analysis, a 3 dB divider is developed (see Fig. 8). Also, as shown in Fig.9, the S-parameters are measured with Agilent E5071B network analyzer are compared with simulated results. It is seen that the division imbalance between S21 and S31 is only 0.03 dB at 4.6 GHz, and it is less than 0.1 dB in the bandwidth of ± 100 MHz. The measured return loss is below -35 dB at 4.6 GHz. The difference between the measured value and the simulated calculation may result from the limitations in the manufacturing accuracy and measuring accuracy.

B. HIGH-POWER TEST

The 4.6 GHz/ 500 kW klystron for EAST is still under development, so the divider has been tested by a 4.6 GHz/ 250 kW klystron. The 4.6 GHz 250 kW test bench is mainly composed of microwave source, transmission line, control and protection system (CPS), and high voltage power supplies (HVPS). Klystron generates 250 kW CW while adding an HVPS, and an optical arcing monitor in transmission line can detect the optical signal, then send an electrical signal to CPS to turn off the microwave source in 5 us while arcing.

To ensure that the divider could work at 500 kW, a 90° phase shifter is connected to port 2, and two short-circuited

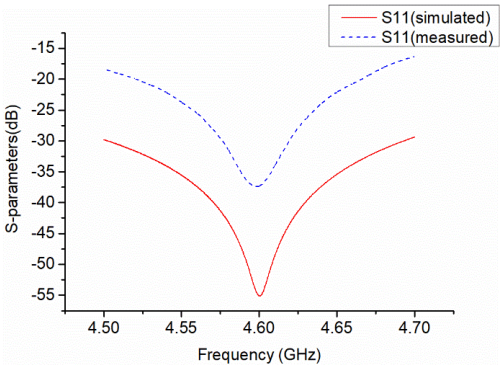

(a)

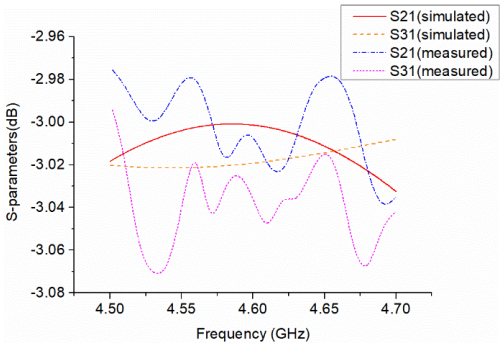

(b)

FIGURE 9. Simulated and measured S-parameters: (a) S11; (b) S21 and S31.

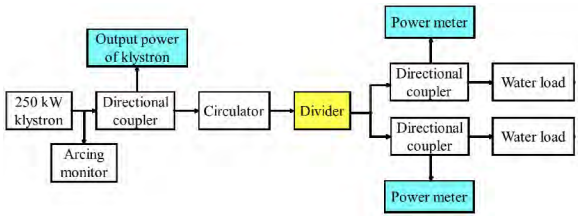

(a)

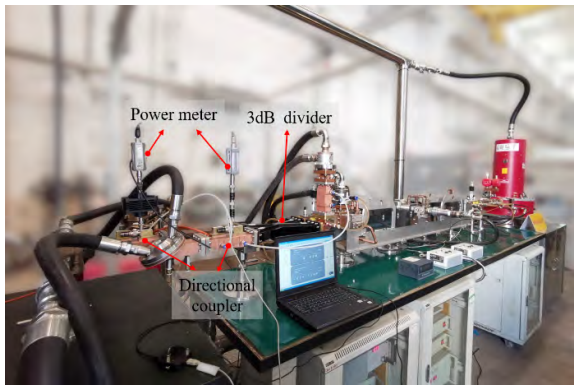

(b)

FIGURE 10. High power testing system of the division ratio test: (a) flow diagrams; (b) photograph.

loads are connected to port 2 and port 3 (see Fig. 11 (b)). Hence, the power arriving at these two ports would reflect fully, and the electric field would be the same as that from

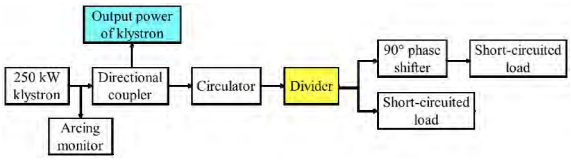

(a)

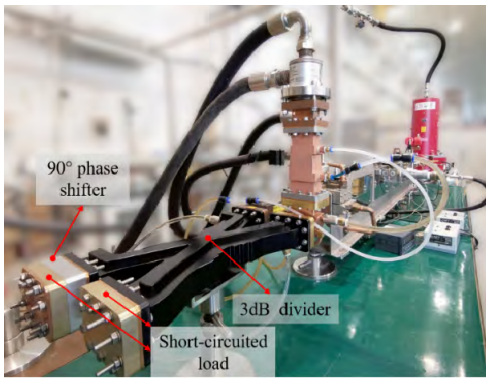

(b)

FIGURE 11. High power testing system of the full reflection test: (a) flow diagrams; (b) photograph.

TABLE 4. Result of the division ratio test when the divider is powered by a 4.6 GHz 250 kW klystron.

Output power of klystron(kW)	Output power of port 2(kW)	Output power of port 3(kW)	Remarks
50	24.1 (-3.17dB)	23.6 (-3.26dB)	-
100	48.6 (-3.13dB)	47.9 (-3.20dB)	-
150	73.4 (-3.11dB)	72.3 (-3.17dB)	-
175	86.1 (-3.08dB)	85.1 (-3.13dB)	-
200	99.2 (-3.05dB)	97.8 (-3.11dB)	-
225	110.5 (-3.09 dB)	109.8 (-3.12dB)	Arced at 220 kW
250 (full power)	123.1 (-3.08dB)	122.3 (-3.11dB)	-

a 500 kW klystron, because of the superposition of the input power and reflected power. The division ratio between S21 and S31 is tested by directional couplers and power meters which are installed at the two output ports separately. The photographs and flow diagrams of the high power test system are plotted in figure 10 and figure 11.

The result of division ratio testing is shown in Table 4 and the output power of klystron are shown in Fig. 12 and Fig. 13.

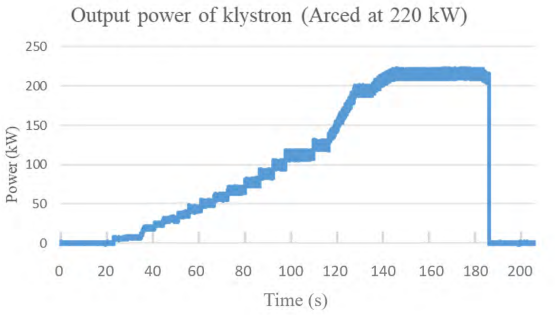

(a)

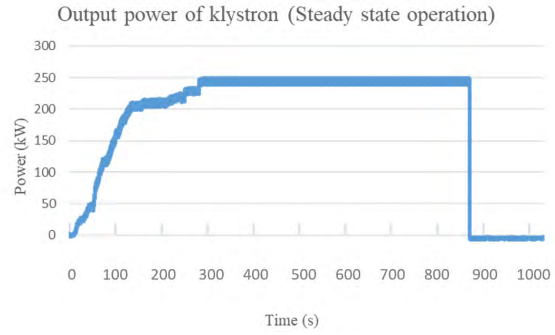

(b)

FIGURE 12. Output power of the klystron during the division test: (a) arced at 220 kW; (b) steady-state operation.

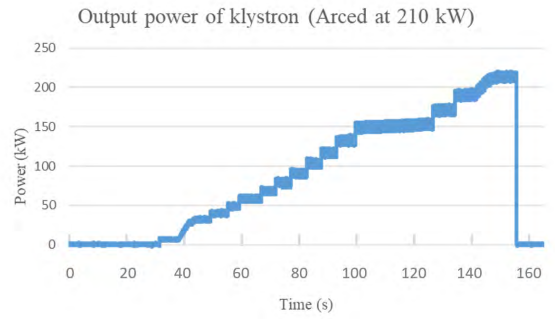

(a)

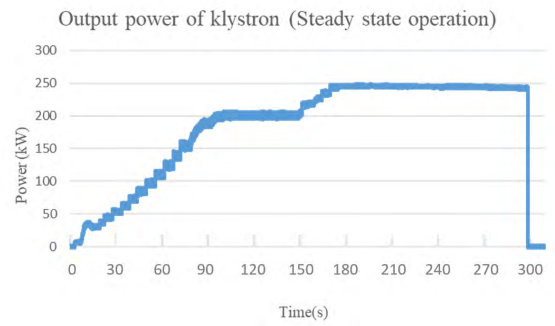

(b)

FIGURE 13. Output power of the klystron during the full reflection test: (a) arced at 210 kW; (b) steady-state operation.

Table 4 shows that the output power of port 2 and port 3 are nearly equal, which is similar to the low power test result. Fig. 12(a) and Fig. 13(a) indicate that the divider has arced

several times, possibly because the inner wall of the divider is not smooth enough, and the burrs were cleared by arcing almost. The divider can work in steady state at 500 kW after conditioning.

IV. CONCLUSION

A high power divider for the 4.6 GHz 500 kW LHCD system on EAST is designed in the combination between microwave theory and thermodynamics. The power capacity can be improved by removing the tuning pin. To solve the heat dissipation problem under high power operation, a water cooling structure is constructed. The tests of the division ratio and the full reflection with 250kW continuous wave have been completed in the high power test bench. Results show that the divider satisfies the design requirements of the LHCD system on EAST.

REFERENCES

[1] Z. Lianmin, S. Jiafang, L. Fukun, J. Hua, W. Mao, L. Liang, W. Xiaojie, and X. Handong, "A 2450 MHz/2 MW lower hybrid current drive system for EAST," *Plasma Sci. Technol.*, vol. 12, no. 1, pp. 118–122, Feb. 2010.

[2] B. Lu, M. Huang, H. Zeng, X. Y. Bai, X. H. Mao, Z. H. Lu, J. Liang, Z. H. Kang, M. W. Wang, K. Feng, and H. Wang, "Development of the 3.7 GHz LHCD system on HL-2A," *J. Korean Phys. Soc.*, vol. 65, no. 8, pp. 1243–1246, Oct. 2014.

[3] Y. L. Chen, B. Lu, X. Y. Bai, J. Liang, C. Wang, H. Zeng, and J. Rao, "Design and measurement of a 3.7 GHz high power recombiner," *Fusion Eng. Des.*, vol. 112, pp. 232–235, Nov. 2016.

[4] Y. M. Jain, P. K. Sharma, H. V. Dixit, A. Jadhav, J. Hillairet, M. Goniche, and J. Kumara, "RF design of Passive Active Multijunction (PAM) launcher for LHCD system of ADITYA-Upgrade tokamak," *Fusion Eng. Design*, vol. 134, pp. 109–117, Sep. 2018.

[5] P. K. Sharma, K. K. Ambulkar, S. Dalakoti, N. Rajanbabu, P. R. Parmar, C. G. Virani, and A. L. Thakur, "High power CW testing of 3.7-GHz klystron for SST1 LHCD system," *IEEE Trans. Plasma Sci.*, vol. 42, no. 9, pp. 2298–2308, Sep. 2014.

[6] H. Do, S. Park, J. H. Jeong, Y. S. Bae, H. L. Yang, L. Delpech, R. Mangne, G. T. Hoang, H. Park, M. H. Cho, and W. Namkung, "Test result of 5 GHz, 500 kW CW Prototype klystron for KSTAR LHCD system," *Fusion Eng. Des.*, vol. 86, nos. 6–8, pp. 992–995, Oct. 2011.

[7] J. Hillairet, J. Achard, C. Brun, S. Rasio, and B. Soler, "Design and testing of a 5 GHz TE_{10}–TE_{30} mode converter mock-up for the lower hybrid antenna proposed for ITER," *Fusion Eng. Des.*, vol. 87, no. 3, pp. 275–280, Mar. 2012.

[8] D. M. Pozar, *Microwave Engineering*, 3rd ed. Hoboken, NJ, USA: Wiley, 2005, ch. 3, pp. 110–121.

[9] E. Pucci, A. U. Zaman, E. Rajo-Iglesias, P.-S. Kildal, and A. Kishk, "Losses in ridge gap waveguide compared with rectangular waveguides and microstrip transmission lines," in *Proc. 4th Eur. Conf. Antennas Propag.*, Barcelona, Spain. Apr. 2010, pp. 1–4.

[10] B. Ravelo and B. Mazari, "Characterization of the regular polygonal waveguide for the RF EM shielding application," *Prog. Electromagn. Res.*, vol. 12, pp. 95–105, 2010.

[11] B. Ravelo, "Modelling of asymmetrical interconnect T-tree laminated on flexible substrate," *Eur. Phys. J. Appl. Phys.* vol. 72, vol. 2, pp. 1–9, Nov. 2015.

[12] J. P. Holman, *Heat Transfer*, vol. 2, 10th ed. New York, NY, USA: McGraw-Hill, 2008, ch. 6, pp. 280–293.

[13] D. Anderson, M. Lisak, and T. Lewin, "Generalized criteria for microwave breakdown in air-filled waveguides," *J. Appl. Phys.*, vol. 65, no. 8, pp. 2935–2945, Aug. 1989.

[14] Y. M. Yang, C.-W. Yuan, and B.-L. Qian, "Measurement of S-band microwave gas breakdown by enhancing the electric field in a waveguide," *IEEE Trans. Plasma Sci.*, vol. 40, no. 12, pp. 3427–3432, Dec. 2012.

[15] C. Chang, G. Liu, C. Tang, C. Chen, and J. Fang, "Review of recent theories and experiments for improving high-power microwave window breakdown thresholds," *Phys. Plasmas*, vol. 18, no. 5, 2011, Art. no. 055702.

[16] C. Vicente, M. Mattes, D. Wolk, B. Mottet, H.L. Hartnagel, J. R. Mosig, and D. Raboso, "Multipactor breakdown prediction in rectangular waveguide based components," in *IEEE MTT-S Int. Microw. Symp. Dig.*, Long Beach, CA, USA, Jun. 2005, p. 4.

[17] S. Anza, C. Vicente, D. Raboso, J. Gil, B. Gimeno, and V. E. Boria, "Enhanced prediction of multipaction breakdown in passive waveguide components including space charge effects," in *IEEE MTT-S Int. Microw. Symp. Dig.*, Atlanta, GA, USA, Jun. 2008, pp. 1095–1098.

DINGZHEN LI was born in Anhui, China, in 1996. He received the B.E. degree in communication engineering from Dalian Maritime University, in 2017. He is currently pursuing the M.S. degree in nuclear science and engineering with the University of Science and Technology of China, with a focus on microwave structure design for LHCD system in EAST.

LIANMIN ZHAO was born in Heilongjiang, China, in 1976. She received the M.S. degree from the Institute of Plasma Physics, Chinese Academy of Sciences (ASIPP), in 2010, where she is currently a Senior Engineer. She is currently involved in the development of the high-power transmission line of the lower hybrid current system on EAST. Her main area of interest is in high-power microwave components and systems.

FUKUN LIU was born in Anhui, China, in 1965. He received the B.S. degree from the Huazhong University of Science and Technology, in 1989. He then joined the Institute of Plasma Physics, Chinese Academy of Sciences, where he is currently a Professor and a Tutor for postgraduate candidates. He is involved in microwave engineering technology and experimental research on plasma physics.

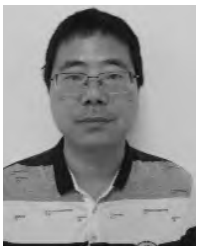

HUA JIA was born in Henan, China, in 1982. He received the Ph.D. degree from the Institute of Plasma Physics, Chinese Academy of Sciences (ASIPP), in 2010, where he is currently an Associate Researcher. He is currently involved in the light emitting plasma system excited by microwave. His main research fields focus on the microwave engineering and plasma physics, microwave systems, and RF energy use.

MIN CHENG was born in Anhui, China, in 1989. He received the B.S. degree from the PLA Artillery College, in 2009. He then joined the Institute of Plasma Physics, Chinese Academy of Sciences. He is involved in microwave engineering technology.

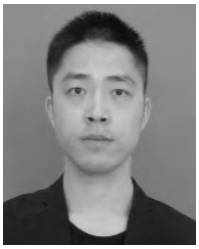

XINSHENG YAN was born in Anhui, China, in 1988. He received the B.S. degree from Northeast Forestry University, in 2011. He is currently pursuing the Ph.D. degree with the University of Science and Technology of China. His research interests include design of microwave resonator and the interaction between microwave and plasma.

TAIAN ZHOU was born in Anhui, China, in 1987. He received the B.E. degree from the Savonia University of Applied Sciences, Finland. He joined the Institute of Plasma Physics, Chinese Academy of Sciences, in 2013. He is involved in microwave engineering technology and water cooling system work.